Original Article

MOLECULAR METABOLISM

Loss of dorsomedial hypothalamic GLP-1 signaling reduces BAT thermogenesis and increases adiposity

Shin J. Lee [1,*], Graciela Sanchez-Watts [2], Jean-Philippe Krieger [1], Angelica Pignalosa [1], Puck N. Norell [1], Alyssa Cortella [2], Klaus G. Pettersen [1], Dubravka Vrdoljak [1], Matthew R. Hayes [3], Scott E. Kanoski [2], Wolfgang Langhans [1,4], Alan G. Watts [2,4]

ABSTRACT

Objective: Glucagon-like peptide-1 (GLP-1) neurons in the hindbrain densely innervate the dorsomedial hypothalamus (DMH), a nucleus strongly implicated in body weight regulation and the sympathetic control of brown adipose tissue (BAT) thermogenesis. Therefore, DMH GLP-1 receptors (GLP-1R) are well placed to regulate energy balance by controlling sympathetic outflow and BAT function.

Methods: We investigate this possibility in adult male rats by using direct administration of GLP-1 (0.5 ug) into the DMH, knocking down DMH GLP-1R mRNA with viral-mediated RNA interference, and by examining the neurochemical phenotype of GLP-1R expressing cells in the DMH using in situ hybridization.

Results: GLP-1 administered into the DMH increased BAT thermogenesis and hepatic triglyceride (TG) mobilization. On the other hand, *Glp1r* knockdown (KD) in the DMH increased body weight gain and adiposity, with a concomitant reduction in energy expenditure (EE), BAT temperature, and uncoupling protein 1 (UCP1) expression. Moreover, DMH *Glp1r* KD induced hepatic steatosis, increased plasma TG, and elevated liver specific de-novo lipogenesis, effects that collectively contributed to insulin resistance. Interestingly, DMH *Glp1r* KD increased neuropeptide Y (NPY) mRNA expression in the DMH. GLP-1R mRNA in the DMH, however, was found in GABAergic not NPY neurons, consistent with a GLP-1R-dependent inhibition of NPY neurons that is mediated by local GABAergic neurons. Finally, DMH *Glp1r* KD attenuated the anorexigenic effects of the GLP-1R agonist exendin-4, highlighting an important role of DMH GLP-1R signaling in GLP-1-based therapies.

Conclusions: Collectively, our data show that DMH GLP-1R signaling plays a key role for BAT thermogenesis and adiposity.

Keywords Neuropeptide; Hypothalamus; Sympathetic nerve; Adipose tissue; Obesity

1. INTRODUCTION

The intestine and brain both produce glucagon-like peptide-1 (GLP-1), which plays an important role in the control of food intake and glycemia [1,2]. GLP-1 producing neurons are primarily located in the nucleus tractus solitarii (NTS) in the hindbrain, where they integrate neural, hormonal, and viscerosensory information arising from meal ingestion [3]. GLP-1 neurons send projections to numerous brain areas involved in the neuroendocrine and autonomic regulation of energy homeostasis [4–6]. Recent studies have highlighted the role of central GLP-1R in mediating the anorexigenic effects of GLP-1R agonists (e.g., exenatide and liraglutide), which are pharmacological treatment options for Type II diabetes and, more recently, obesity [7–11]. Intracerebroventricular injection of GLP-1 or GLP-1R agonists decreases food intake and increases energy expenditure (EE) [12–14], resulting in weight loss.

The recent emergence of GLP-1's role in the control of the sympathetic nervous system (SNS) highlights novel mechanisms through which GLP-1 contributes to energy balance [15]. Stimulation of central GLP-1R increases brown adipose tissue (BAT) thermogenesis and causes weight loss in a way that is largely independent of its anorexigenic effects [14,16–19]. Central GLP-1 infusion also decreases de-novo lipogenesis in the liver and hepatic as well as adipose tissue triglyceride content [20,21]. It is unknown, however, whether central GLP-1R-mediated effects on sympathetic regulation of adipose tissue and liver are associated with the pathogenesis of obesity and insulin resistance. A recent study showed that GLP-1R expression is reduced in postmortem hypothalamic nuclei of obese diabetic humans [22], suggesting that reduced hypothalamic GLP-1R signaling may contribute to the development of the metabolic syndrome.

The dorsomedial nucleus of the hypothalamus (DMH), a key part of the sympathetic control network [23], expresses GLP-1R and is densely

[1]Physiology and Behavior Laboratory, ETH Zürich, 8603 Schwerzenbach, Switzerland [2]Department of Biological Sciences, University of Southern California, Los Angeles, CA 90089, USA [3]Department of Psychiatry, Perelman School of Medicine at the University of Pennsylvania, Philadelphia, PA, USA

[4] Co-senior authors.

*Corresponding author. Physiology and Behavior Laboratory, ETH Zürich, 8603 Schwerzenbach, Switzerland. E-mail: shin-lee@ethz.ch (S.J. Lee).

Received February 6, 2018 • Revision received March 9, 2018 • Accepted March 14, 2018 • Available online 21 March 2018

https://doi.org/10.1016/j.molmet.2018.03.008

innervated by GLP-1 fibers [4,5,24,25], suggesting a possible role of DMH GLP-1R signaling in SNS regulation. DMH neurons send monosynaptic projections to the rostral raphe pallidus (rRPa), which contains sympathetic premotor neurons regulating BAT activity [26–29]. Disinhibiting DMH glutamatergic neurons stimulates BAT sympathetic nerve activity (SNA) and thermogenesis [30,31]. Moreover, the DMH mediates increased blood pressure and heart rate during psychogenic stress [32] and obesity [33]. DMH leptin receptor (LEPR) expressing neurons have been synaptically and functionally linked to BAT thermogenesis [34–36]. Blocking or ablating DMH LEPR reduced EE and the thermogenic effects of leptin [34,35]. Similar to LEPR in the DMH [37], GLP-1R are expressed in the anterior and ventral part of the DMH [5,38]. However, the neurochemical phenotype and function of GLP-1R expressing neurons are unknown. Given the changes in GLP-1R expression observed in the hypothalamus of obese diabetic humans [22], a decrease in DMH GLP-1R signaling may also play an important role in the pathogenesis of obesity via a SNS-dependent mechanism. Neuropeptide Y (NPY) expressing neurons in the DMH have long been implicated in controlling ingestive behavior and body weight (BW) [39–43]. Knockdown of DMH *NPY* expression decreases food intake, reduces fat mass, and ameliorates diet-induced obesity (DIO) and insulin resistance [44–46]. Interestingly, DMH *NPY* knockdown also increases BAT thermogenesis and white adipose tissue (WAT) browning, suggesting that DMH NPY neurons contribute to the development of obesity, in part by decreasing sympathetic outflow [47]. However, the mechanisms through DMH NPY neurons reduce sympathetic outflow are poorly understood. Arcuate nucleus (ARC) NPY neurons are inhibited by local GLP-1-sensitive GABAergic neurons [9], raising the possibility that a similar mechanism may contribute to DMH NPY neuronal regulation.

Here we investigate the role of DMH GLP-1R signaling in the sympathetic regulation of BAT in male rats by assessing 1) the short-term effects of DMH GLP-1 injections on BAT thermogenesis, 2) the effects of long-term DMH *Glp1r* knockdown (KD) on BW, EE, BAT thermogenesis, and glucose metabolism, and 3) the neurochemical identity of DMH GLP-1R expressing neurons. We found that DMH GLP-1R stimulation increased BAT thermogenesis and hepatic fuel mobilization, whereas DMH *Glp1r* KD increased adiposity, decreased EE, impaired BAT function, and hepatic steatosis; effects which collectively contributed to increased insulin resistance and blunted the anorexigenic response to the long-lasting GLP-1R agonist, exendin-4 (Ex-4). In addition, DMH *Glp1r* KD locally increased *NPY* expression, implicating NPY as a downstream substrate for DMH neuronal regulation of BAT thermogenesis. Collectively, our results show that DMH GLP-1R signaling is a physiologically important component of the central GLP-1 system that controls BAT thermogenesis in a way that helps maintain energy balance.

2. MATERIALS AND METHODS

2.1. Animals

Male Sprague Dawley (SD) rats were purchased from Charles River Laboratories (Sulzfeld, Germany) or Harlan (Envigo US) and housed individually in a climate-controlled room (temperature: 23 ± 2 °C, humidity: 55 ± 5%). Rats were maintained on a 12 h/12 h light/dark cycle with ad libitum access to standard chow diet (No 3436, Provimi Kliba AG, Kaiseraugust, Switzerland) and tap water, except as noted. All procedures were approved by the Cantonal Veterinary Office of Zurich, or the University of Southern California Institutional Animal Care and Use Committee.

2.2. Stereotaxic surgery

SD rats (320–340 g; pre-surgical BW) were anesthetized by intraperitoneal injection of 2 mg/kg Xylazine (Rompun 2%, Provet AG, Lyssach, Switzerland) and 10 mg/kg BW Ketamin (Ketalar 50 mg/ml, Pfizer AG, Zurich, Switzerland), and positioned in the stereotaxic apparatus.

Acute DMH GLP-1R activation study: Bilateral guided cannulas (Bilaney, Dusseldorf, Germany) were positioned immediately above the DMH (3.3 mm caudal to the bregma, 1 mm from center to center, 8 mm below pedestal). Sham injections started after 7 days of recovery (injectors fit to 8 mm guided cannula with 1.5 mm projections). On the experiment day, GLP-1 (0.5 ug in 0.5 ul volume, n = 8) or saline (0.5 ul, n = 8) was injected bilaterally 4 h after dark onset. The placement of the cannula was verified during cryosectioning the brains.

DMH Glp1r knockdown: AAV-GFP or AAV GLP-1R shRNA constructs were previously described in detail [48,49]. 200 nl of AAV-GFP or AAV GLP-1R shRNA (5.22 e12 GC/ml) was bilaterally injected into the DMH (3.3 mm caudal, 0.5 mm lateral to the bregma, and 8.4 mm ventral to dura) using a glass capillary micropipette connected with polyethylene (PE)-tubing to a microinjector (Picospritzer III, Parker Hannifin, Hollis, USA). All injected rats (n = 7 for AAV-GFP and n = 10 for AAV GLP-1R) were also implanted with intraperitoneal catheters for subsequent drug injections. Food intake and BW were measured daily. Behavioral and metabolic effects were assessed beginning approximately 3 weeks after surgery. Only the animals with bilateral GFP expression within the DMH were included in the final analyses.

2.3. Indirect calorimetry

Respiratory exchange ratio (RER) and energy expenditure (EE) measurements were conducted in an open circuit calorimetry Phenomaster system (TSE) after 3 days of habituation. TSE Indirect calorimetry estimates EE (kcal/h/kg) from the animals's O2 consumption (mL/kg/h) and CO2 production (mL/kg/h) using the Weir equation [50,51]. RER: VCO2/VO2. EE: $(3.941 \times VO2 + 1.106 \times VCO2)/1000$. For the *Glp1r* KD study, RER and EE were measured at 8 weeks after surgery. For the acute study, RER and EE were measured before and after intra-DMH GLP-1 (Bachem, 0.5 μg in 0.5 μl saline, n = 8) or vehicle (n = 8) administration for comparison. Data are presented as the average RER and EE values in dark, light, and total diurnal cycle for 3 consecutive days.

2.4. BAT and core temperature measurements

Infra-red (IR) pictures were taken with an E60 camera (FLIR), mounted vertically over the shaved interscapular area (distance 30 cm). Rats were lightly restrained in a stretched position under the camera and 3 snapshots/time point were taken for further analysis. For the acute study, baseline IR pictures were taken prior to intra-DMH vehicle/GLP-1 injection (0.5 μg in 0.5 μl saline) and a second series of IR pictures was taken 4 h after the injection. Body core temperature was measured with a rectal thermometer (WD-35427-20, Oakton instruments) before and 4 h after the injection. For the *Glp1r* KD study, all rats were subjected to BAT IR recording 5 h after dark onset at 4 weeks. For the β-3 receptor agonist study, rats had ad lib access to food for 2 h after dark onset. After 1.5 h of fasting, rats received 1 ug/kg IP injection of β-3 receptor agonist (Sigma–Aldrich CL316243) or PBS. IR pictures were taken 2 h after the injection. Final analyses of the IR pictures were done by defining a standard rectangular area (60 × 20 px) over the interscapular region and averaging the mean area temperatures of two pictures (FLIR Tool software for PC).

2.5. Measurement of food intake and body composition

Daily food intake and meal patterns were recorded by an in-house automated system [52]. For the fast-refeeding study, the rats were fasted for 24 h prior to refeeding. Food intake was measured at 0.5, 1, 2, 4, and 6 h after dark phase onset. Analysis of body composition was conducted using a computerized tomography system (La Theta LCT-100, Aloka) with a previously validated method [53] Briefly, rats (AAV GLP-1R n = 10 and AAV-GFP n = 7) were anesthetized with isoflurane and placed supine in a cylindric holder (120 mm inner diameter). An initial whole-body sagittal image was obtained to ensure proper placement of the animal. Scans were done from vertebrae L1 to L6 with a 2 mm pitch size. The Aloka software detects volumes of adipose tissue (fat mass), bone, air, and the remainder (lean mass) based on their X-ray absorption. Fat mass and lean mass were computed using the density factors of 0.92 g/cm^3 and 1.10 g/cm^3, respectively. Fat ratio is defined as fat mass/(lean + fat mass).

2.6. Intraperitoneal glucose tolerance test (IPGTT)

All rats (AAV GLP-1R n = 10 and AAV-GFP, n = 7) were fasted overnight and injected with 2 g/kg glucose (IP). Tail vein blood was collected at 0, 15, 30, 60, 90, and 120 min after the glucose bolus injection.

2.7. Systemic Exendin-4 effects on FI, BW, and EE

On the day of the experiment, all rats (AAV GLP-1R n = 10 and AAV-GFP n = 7) were fasted for 4 h and received either Ex-4 (1.0 μg/kg, IP) or saline at dark cycle onset. RER and EE measurements were conducted in an open circuit calorimetry Phenomaster system (TSE) for 24 h after drug injection. Food intake and BW were measured at 24 h after drug injection.

2.8. Tissue morphology

For stainings with hematoxylin and eosin (H&E) and oil red O (ORO) adipose and liver tissues were fixed in 4% PFA (Sigma–Aldrich) and processed in a STP 120 (Microm) according to the standard protocol. Paraffin-embedded samples were cut at 5 μm on a Hyrax M55 (Zeiss), deparaffinized and stained on a Varistain 24-4 (Shandon) for adipose tissue or ORO (Sigma–Aldrich, cat # 00625) for liver [54]. Pictures were obtained with an Axioscope A.1 microscope (Zeiss). H&E and ORO images were quantified for lipid fraction and ORO area using ImageJ software.

2.9. Plasma analysis

Triglycerides, FFA, glycerol, and cholesterol levels were analyzed by Cobas MIRA autoanalyzer [63] (Hoffman LaRoche, Basel, Switzerland). Insulin and leptin levels were measured by using a Multi-Array Mouse/Rat Insulin and leptin kit (Meso Scale Discovery, Gaithersburg, USA).

2.10. Gene expression analyses

For the gene expression analyses in the acute DMH-GLP-1R activation study, rats were decapitated 4 h after the DMH injections of GLP-1 (0.5 μg in 0.5 μl saline) or vehicle. Brains and BAT were collected, frozen in dry ice and stored at −80 °C for RNA extraction. For the KD study, brains, liver, BAT, and WAT were collected, frozen in dry ice and stored at −80 °C for RNA and protein extraction. DMH, PVH, and ARC were micropunched using anatomical landmarks and RNA was extracted using Trizol (Life Technologies) according to the manufacturer's protocol. RT-qPCR was performed using SYBR green on a OneStep Plus Real Time PCR instrument (Applied Biosystems) and results were analyzed using the 2ddCt method (all primer sequences available upon request).

2.11. Western blot analyses

Western blots were performed using a protocol previously described in detail [64]. Briefly, proteins were separated by 8–10% SDS -polyacrylamide gel polyacrylamide electrophoresis and transferred onto nitrocellulose membranes (pore size 0.2 μm; Protran, Whatman). Membranes were then blocked in 5% skim milk in Tris-buffered saline containing 0.1% Tween-20 for 1 h before incubating with the primary antibodies overnight at 4 °C. On the next day, the membranes were washed 3 times with Tween-20, and incubated with secondary horseradish peroxidase-conjugated anti-rabbit or anti-mouse IgG, respectively, for 1 h at RT. Protein bands were visualized using a chemiluminescent substrate and the intensities of the bands were quantified by densitometry using Image J software (ImageJ 1.46b). Primary antibodies: Uncoupling protein 1 (UCP1; Rabbit antibody PA1-24894 1:2000, ThermoFisher), ACC (Rabbit antibody 3662, 1:1000, Cell Signaling), pACC (Rabbit antibody 3661, 1:1000, Cell Signaling), FAS (Rabbit antibody 3180, 1:1000, Cell Signaling), β-actin (Mouse antibody AC-74, 1:5000, Sigma–Aldrich), γ-tubulin (Mouse antibody T6557, 1:5000, Sigma–Aldrich).

2.12. In situ hybridization

2.12.1. Animals for in situ hybridization

Five male Sprague–Dawley rats (BW 275–300 g) were anesthetized and perfused through the ascending aorta with ice-cold 4% paraformaldehyde in 0.1 M sodium tetraborate (pH 9.5) as previously described [55]. Brains were removed and post-fixed for 24 h in the borate fixative containing 12% sucrose, frozen in hexanes cooled with dry ice, and then stored at −70 °C. Five series of one in five, 20 μm thick, frozen coronal sections were cut through the hypothalamus in the same approximate plane as the Swanson Rat Brain Atlas [56] and mounted on Superfrost Plus slides the same day, stored overnight under vacuum and then desiccated at −70 °C. One series was stained with thionin for local cytoarchitectonics.

We used two in situ hybridization (ISH) procedures to assess how GLP-1R mRNA was related to other key neuronal mRNAs in the DMH. First, single ^{35}S cRNA ISH was used to survey the rostrocaudal distribution of VGluT2, GAD 65, NPY, and GLP-1R mRNAs. To determine the chemical identity of DMH neurons containing GLP-1R mRNA we then used two double ISH methods: a ^{35}S-labeled and digoxigenin fluorescence ISH (FISH) modified from Watts & Sanchez-Watts [57], and Advanced Cell Diagnostics RNAscope® Multiplex FISH [58].

2.12.2. In situ hybridization

Antisense cRNA probes for VGluT2 [59], GAD 65 [60], NPY [61], and GLP-1R [62] mRNAs were transcribed using either ^{35}S-UTP or a Digoxigenin RNA labeling mix (Roche) as previously described with minor modifications [57].

^{35}S-In situ hybridization: Single ^{35}S cRNA ISH was performed using all 4 probes as previously described [55].

Combined ^{35}S- and digoxigenin-labeled (ISH/FISH): An optimized mixture of either ^{35}S-labeled NPY or GAD65 cRNA probe was cocktailed with the DIG-labeled GLP-1R cRNA probe and used for ISH as previously described with minor modifications [57]. Slide-mounted sections were exposed to Agfa Mamoray HDR-C film for 4 days to estimate the exposure time required for emulsion autoradiography for the ^{35}S hybridization. To visualize the digoxigenin-RNA the same slides were processed with the HNPP Fluorescent Detection Kit (Roche) modified from the manufacturer's protocol. Slides were incubated in blocking buffer containing 0.05% Triton-100/2% Normal Sheep Serum/2X SSC for 2.5 h at 30 °C, rinsed in Digoxigenin Buffer 1

(100 mM Tri-HCl/150 mM NaCl pH 7.5) and then incubated overnight at 4 °C in Anti-Digoxigenin-AP Fab fragments diluted 1:3 K with Digoxigenin Buffer 1/0.3% Triton-100/1% Normal Sheep Serum, and then washed in Digoxigenin Buffer 3 (Washing Buffer: 0.05% Tween 20/Digoxigenin Buffer 1) followed by Digoxigenin Buffer 4 (Detection Buffer: 100 mM Tris-HCl/100 mM NaCl/10 mM $MgCl_2$ pH 8). To reveal a specific fluorescent signal, a Fast Red TR solution was prepared first at a concentration of 25 mg/ml in redistilled water. The final mixture contained 10 μl Fast Red solution and 10 μl HNPP per ml of Digoxigenin Buffer 4 (Detection Buffer pH 8). The HNPP/Fast Red TR mixture was filtered through a 0.2 mM nylon syringe filter immediately before use. 90 μl of filtered HNPP/Fast Red TR mix was applied to each slide, coverslipped and incubated in the dark at 25 °C for 30 min then washed in Digoxigenin Buffer 3. These two steps were repeated 3 times before slides were rinsed in distilled water and air dried in the dark.

To visualize ^{35}S-labeled cRNA hybridization, slides were dipped in Kodak autoradiography emulsion type NTB (diluted 1:1 with distilled water), exposed for 4 days (GAD65) and 12 days (NPY), developed with D19 & Rapid Fix, allowed to air dry in the dark, and then coverslipped with DABCO.

Fluorescent (RNAscope®) in situ hybridization (FISH) for GLP-1R, NPY, GAD65, and vGluT2 mRNAs: Slide-mounted sections from the same animals used for the combined ^{35}S- and digoxigenin-labeled (ISH/FISH) were processed to detect the mRNAs for GLP-1R (ACD 315221), NPY (ACD 413191), GAD65 (ACD 435801-C2), and VGlut2 (ACD 317011-C2) using RNAscope® Multiplex FISH, modified from Hsu et al. [58].

2.12.3. Image analysis

Sections were photographed with a Zeiss Axioimager Z1 epifluorescence microscope through a 5× or 10× plan-apochromat objective lenses. Dark field illumination to visualize silver grains was provided by a Microvid lateral illumination system (Micro Video Inc., Avon MA). Fluorescence and dark field images of the same field were captured with a Hamamatsu Orca ER monochromatic digital camera controlled with Volocity 6.1 software (Perkin Elmer, Waltham, MA). All photoimages were then imported into Adobe Photoshop (CS3; Adobe Systems, Inc., San Jose, CA), and the fluorescence and dark field images were merged using separate Photoshop layers. All figure panels were assembled in Adobe Illustrator (CS3) to identify double-labeled neurons.

2.13. Statistical analyses

Data were analyzed by a Student's t-test for unpaired normally distributed values of equal variance using GraphPad Prism (version 6.05 for Windows). Where the dependent variable was affected by two factors, the data were analyzed with a 2-way ANOVA. When the main effect—or interaction terms were significant, post-hoc analyses using the Bonferroni correction were performed. Data are presented as means ± SEM. *P*-values < 0.05 were considered significant. All graphs were generated using GraphPad Prism (version 6.05 for Windows).

3. RESULTS

3.1. Acute DMH GLP-1R stimulation increases BAT thermogenesis

We injected GLP-1 (0.5 ug) bilaterally into the DMH and measured BAT temperature under a special feeding schedule to standardize food intake (Figure 1A), thereby isolating the effects of GLP-1R activation on BAT thermogenesis. DMH GLP-1R stimulation increased interscapular BAT temperature (Figure 1B,C, $p < 0.001$) and core body temperature (Figure 1D, $p < 0.05$) at 4 h after injection. In support of increased BAT temperature, mRNA expression of β3-adrenergic receptor (ADRB3, $p < 0.05$), peroxisome proliferator-activated receptor gamma coactivator 1-alpha (PGC1α, $p < 0.05$), peroxisome proliferator-activated receptor gamma (PPARγ, $p < 0.05$), and cell death-Inducing DFFA-like effector A (CIDEA, $p < 0.05$) was up-regulated in the BAT at 4 h after GLP-1 injection (Figure 1E). There was, however, no significant change in uncoupling protein 1 (UCP1) mRNA expression in the BAT. DMH GLP-1 injection also increased respiratory exchange ratio (RER, Figure 1F, $p < 0.05$) but did not affect EE (S1A). BAT thermogenesis requires fatty acids as fuel for heat generation [65]. Interestingly, acute DMH GLP-1R stimulation increased TG levels in the plasma (Figure 1G, $p < 0.05$) as well as liver fatty acid synthase (FAS) gene expression (Figure 1H, $p < 0.05$). Free fatty acids (FFA), glycerol, and β-hydroxybutyrate (BHB) levels were unchanged in the plasma of GLP-1 injected rats (S1B). DMH GLP-1R stimulation led to a decrease in NPY ($p < 0.05$) mRNA expression, but did not significantly affect GLP-1R and cocain- and amphetamine-regulated transcript (CART) mRNA expression (Figure 1I), raising the possibility that inhibition of NPY gene expression by GLP-1 is involved in the sympathetic control of BAT thermogenesis.

3.2. Long term DMH *Glp1r* KD increases adiposity

To further examine the role of DMH GLP-1R in BW homeostasis, we generated a rat model of *Glp1r* KD specifically in the DMH using viral-mediated RNA interference (Figure 2A). Rats injected with AAV-GLP-1R shRNA showed a significant reduction (51%) of GLP-1R mRNA (Figure 2B, $p < 0.001$) expression in the DMH compared to rats injected with AAV-Control shRNA expressing GFP only. GLP-1R mRNA expression in the ARC and PVH was not affected by viral injection (Figure 2B). We also found a partial reduction of GLP-1R protein expression in the DMH (S2A, $P = 0.05$). Starting at 7 weeks after viral infection, AAV-GLP-1R rats displayed a small, but significant increase in BW gain compared to controls (Figure 2C, $p < 0.05$, BW in S2B). This BW gain was accompanied by an increase in fat mass (Figure 2D, $p < 0.01$) and an upward trend in fasting leptin levels (Figure 2E, $p = 0.09$). Food intake was not different between the two groups during the first 4 weeks post injection (Figure 2F). Despite the lack of a change in initial daily food intake, AAV-GLP-1R rats displayed an abnormal meal pattern, i.e., a decrease in meal size and an increase in meal number during the dark phase (S2C—I). Furthermore, AAV-GLP-1R rats reduced refeeding response (Figure 2G, $p < 0.001$), and BW change (Figure 2H, $p < 0.05$) to 24 h fasting. In addition, DMH *Glp1r* KD reduced adrenal gland weight, an indicator of altered sympathetic activity (S3A).

3.3. Long term DMH *Glp1r* KD decreases EE, BAT temperature, and UCP1 expression

Consistent with increased adiposity, DMH *Glp1r* KD rats exhibited reduced EE during the dark phase, but not during the light phase (Figure 3A,B, $p < 0.001$). On the other hand, RER was not different between AAV-GLP-1R and AAV-Control rats (Figure 3C,D). BAT temperature was significantly lower in AAV-GLP-1R rats compared to the controls (Figure 3E, $p < 0.05$), indicating low thermogenic capacity as a result of long term *Glp1r* KD. Core temperature was however not different between the two groups (Figure 3F). β-3 adrenergic receptor stimulation by CL- 316243 (0.1 mg/kg, SC) increased BAT temperature in the controls (Figure 3G, $p < 0.005$), but not in AAV-GLP-1R rats. Consistently, adipocytes were bigger in the BAT of AAV GLP-1R rats than in controls (Figure 3H, $P < 0.05$), indicating lipid accumulation in the cells. We hypothesized that DMH *Glp1r* KD blunts the stimulatory effect of β-3 adrenergic receptor agonist due to chronic reduction in

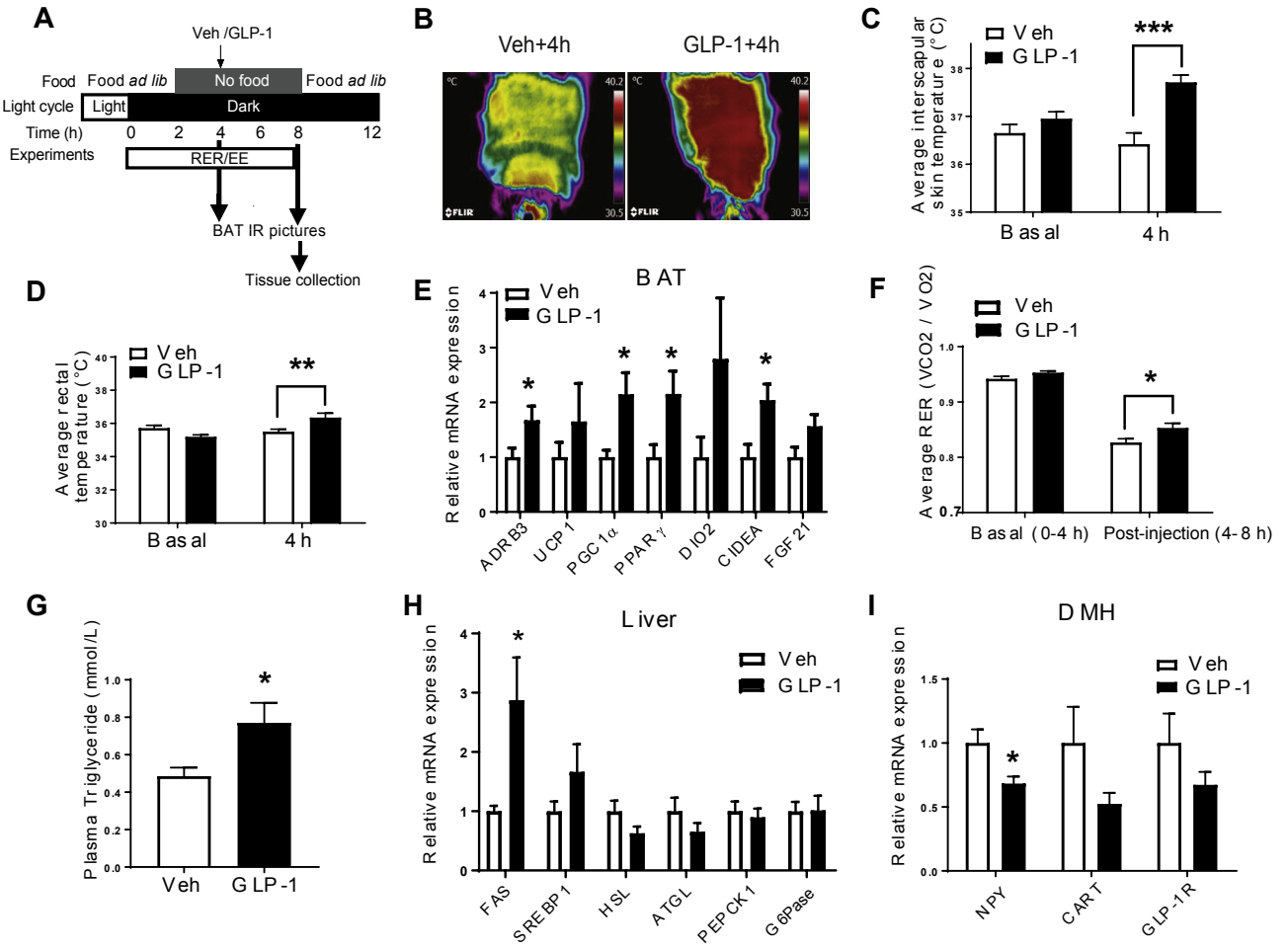

Figure 1: DMH GLP-1R stimulation increases BAT thermogenesis and TG mobilization from liver. (A) Experimental protocol. **(B, C)** Representative infrared pictures of the interscapular area before and 4 h after Veh or GLP-1 (0.5 μg) injection into the DMH ($n = 7–8$; Two-way ANOVA; ***$p < 0.0001$). **(D)** Rectal temperature ($n = 7/8$; Two-way ANOVA; **$p < 0.005$). **(E)** Relative mRNA expression in the BAT: $n = 7/7$; Student t-tests; *$p < 0.05$ for ADRB3, CIDEA, PGC1α, PPARγ, ns ($p > 0.05$): UCP1, iodothyronine deiodinase 2 (DIO2), and FGF21. **(F)** Respiratory exchange ratio before (basal: 0–4 h after dark onset) and after (post injection:4–8 h after dark onset) Veh or GLP-1 injection into the DMH ($n = 7/7$; Two-way ANOVA; *$p < 0.05$). **(G)** Plasma TG levels ($n = 7/8$; Student t-test; *$p < 0.05$). **(H)** Relative mRNA expression in liver: $n = 7/7$; Student t-tests; *$p < 0.05$ for FAS. ns: sterol regulatory element-binding protein 1(SREBP1), HSL, ATGL, PEPCK1, and G6Pase. **(I)** Relative mRNA expression in the DMH: $n = 7/7$; Student t-test; *$p < 0.05$ for NPY. ns: CART and GLP-1R. Data are mean ± SEM.

SNS outflow to brown adipocytes supressing the cellular machineries critical for thermogenesis. In fact, AAV-GLP-1R rats had lower levels of UCP1 mRNA (Figure 3I, $P < 0.005$) and protein (Figure 3J, $P < 0.01$) in BAT, together with lower expression levels of other thermogenic genes including PGC1α ($p < 0.05$) and PPARγ ($p < 0.05$) in the BAT(Figure 3I). Together, these data show that reduced EE and BAT thermogenesis contributed to increased adiposity in DMH *Glp1r* KD rats.

3.4. Long term DMH *Glp1r* KD impairs lipid and glucose metabolism

Consistent with increased adiposity, plasma triglyceride levels were higher in AAV GLP-1R rats compared to controls (Figure 4A, $p < 0.005$), but cholesterol, free fatty acid, and glycerol levels were comparable between the two groups (S3B–D). Oil red O staining revealed lipid accumulation in the livers of AAV-GLP-1R rats (Figure 4B, $p < 0.001$), further supported by the activation of *de novo* lipogenesis genes (Figure 4C). DMH *Glp1r* KD resulted in increased fatty acid synthase (FAS, $p < 0.05$) and a tendency of increased acetyl-CoA carboxylase (ACC, $p = 0.06$) gene expression. Similarly, FAS and ACC protein levels were higher in AAV-GLP-1R rats (Figure 4D, $p < 0.05$). pACC protein expression and pACC/ACC ratio were however unchanged. On the other hand, DMH *Glp1r* KD decreased glucose 6-phosphatase (G6Pase, $p < 0.005$) and phosphoenolpyruvate carboxykinase 1 (PEPCK1, $p < 0.01$), indicating decreased gluconeogenesis, presumably due to increased insulin production (Figure 4C). The expression of fibroblast growth factor 21 (FGF21) and PGC1α in the liver was similar in the two groups (Figure 4C). Unlike its expression in liver, FAS mRNA expression was down-regulated in the subcutaneous white adipose tissue (scWAT, Figure 4 E, $p < 0.05$). There was no change in the mRNA expression of lipolytic enzymes, adipose triglyceride lipase (ATGL) and hormone-sensitive lipase (HSL), in the scWAT of AAV-GLP-1R rats. Although DMH *Glp1r* KD did not affect the glucose profile during an intraperitoneal glucose tolerance test (IPGTT) at 7 weeks post viral injection (Figure 4 F), insulin secretion in response to the glucose challenge was greater in AAV-GLP-1R rats than in controls (Figure 4G, $p < 0.05$), suggesting that AAV-GLP-1R rats are more insulin resistant. Becasue BW gain was higher in AAV-GLP-1R rats, this decrease in insulin sensitivity may be secondary to

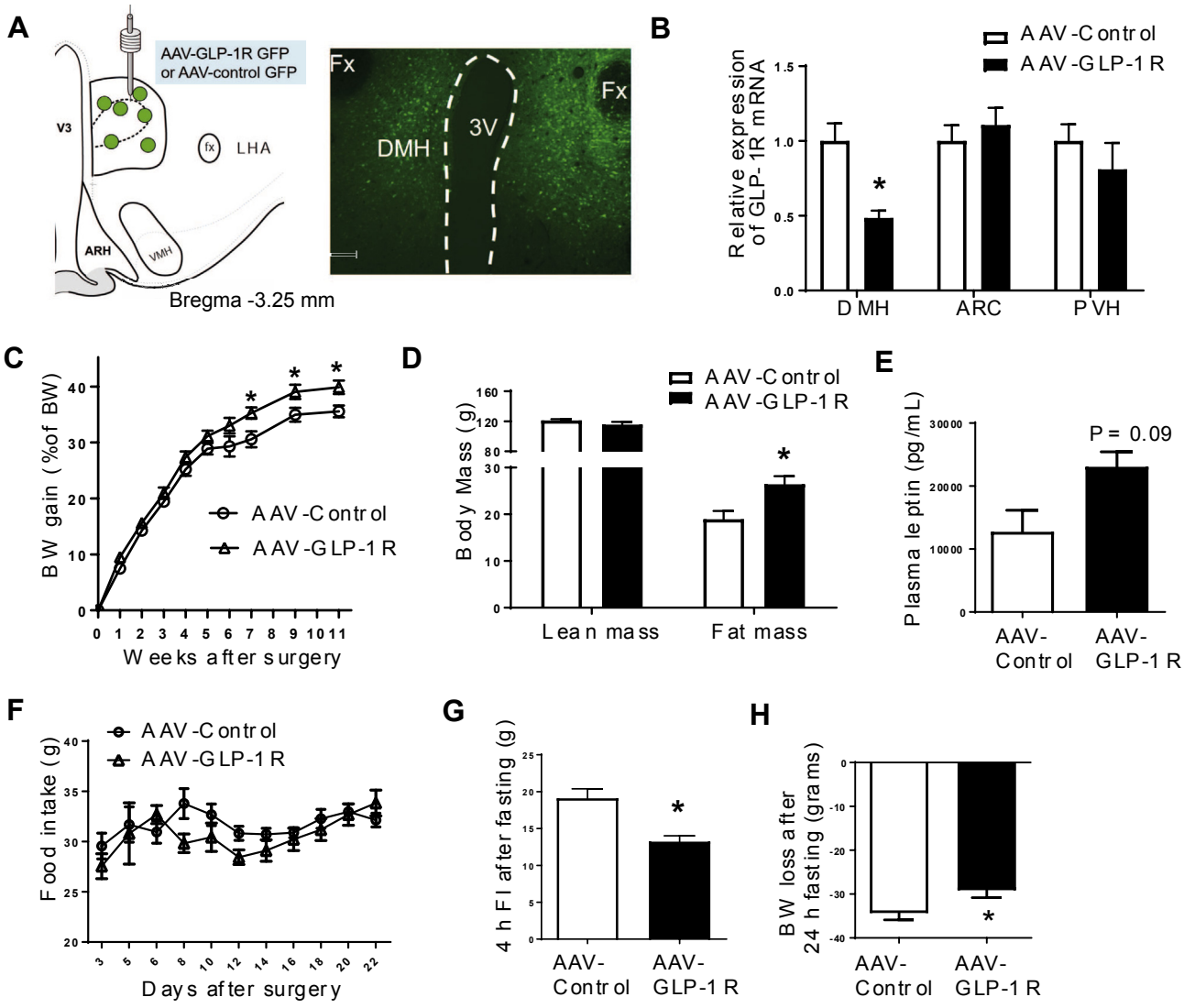

Figure 2: DMH *Glp1r* KD increases BW gain and adiposity. (A) Illustration of AAV injection site and GFP infected cells in the DMH. **(B)** Relative GLP-1R mRNA expression in the DMH, ARC, and PVH (n = 6/8; Student t-tests; *p < 0.001 for DMH). **(C)** BW gain (as % of BW) of AAV-control and AAV-GLP-1R rats on standard chow diet for 11 weeks (n = 7/9; Student t-tests; *p < 0.05). **(D)** Lean and fat mass of AAV-control and AAV-GLP-1R rats (n = 7/9; Student t-tests; *p < 0.01). **(E)** Plasma leptin levels (n = 6/6; Student t-test; p = 0.09). **(F)** Daily food intake of AAV-control and AAV-GLP-1R rats for 22 days after surgery. **(G)** 4 h food intake after 24 h fasting (n = 7/9; Student t-test; *p < 0.001). **(H)** BW change after 24 h fasting (n = 7/9; Student t-test; *p < 0.05). Data are mean ± SEM.

the change in BW gain rather than a direct effect of KD. In addition, the fasting insulin level was higher in AAV-GLP-1R rats compared to the controls (Figure 4H, $p < 0.05$). Together, these results indicate that *Glp1r* KD in the DMH alters lipid metabolism in liver and adipose tissue, which is associated with insulin resistance.

3.5. Long term DMH *Glp1r* KD increases DMH NPY mRNA expression

In contrast to DMH GLP-1R stimulation, DMH *Glp1r* KD increased NPY mRNA expression in the DMH (Figure 5A, $p < 0.001$), providing further support for the regulation of NPY transcription by GLP-1R signaling. The leptin receptor (LEPR) in the DMH also regulates BAT thermogenesis [36]. We did, however, not detect a change in either LEPR, the cholecystokinin receptor (CCKR), or CART expression in the DMH of AAV-GLP-1R rats. Because DMH NPY neurons send major projections to the PVH [28], it is possible that NPY regulates BAT thermogenesis via modulating gene expression in the PVH [66]. While there were no statistically significant changes in thyrotropin releasing hormone (TRH) and CART mRNA levels after knocking down DMH GLP-1R mRNA, there were trends towards changes in corticotropin releasing hormone (CRH) and tyrosine hydroxylase (TH, $p = 0.07$) mRNAs (Figure 5B). Interpreting these results conservatively therefore leaves open the possibility that DMH NPY projections to the PVH can in some way influence the autonomic and neuroendocrine regulation of energy balance. Levels of proopiomelanocortin (POMC), agouti-related protein (AgRP), NPY, and CART mRNAs were not different between the two groups in the ARC (Figure 5C).

3.6. DMH-GLP-1 neurons express GAD65 but not NPY mRNAs

To determine the neurotransmitter identity of the DMH neurons containing GLP-1R mRNA, we used two in situ hybridization techniques that can detect multiple mRNAs simultaneously. GLP-1R mRNA-containing neurons were found throughout the rostrocaudal extent of the DMH (S4).

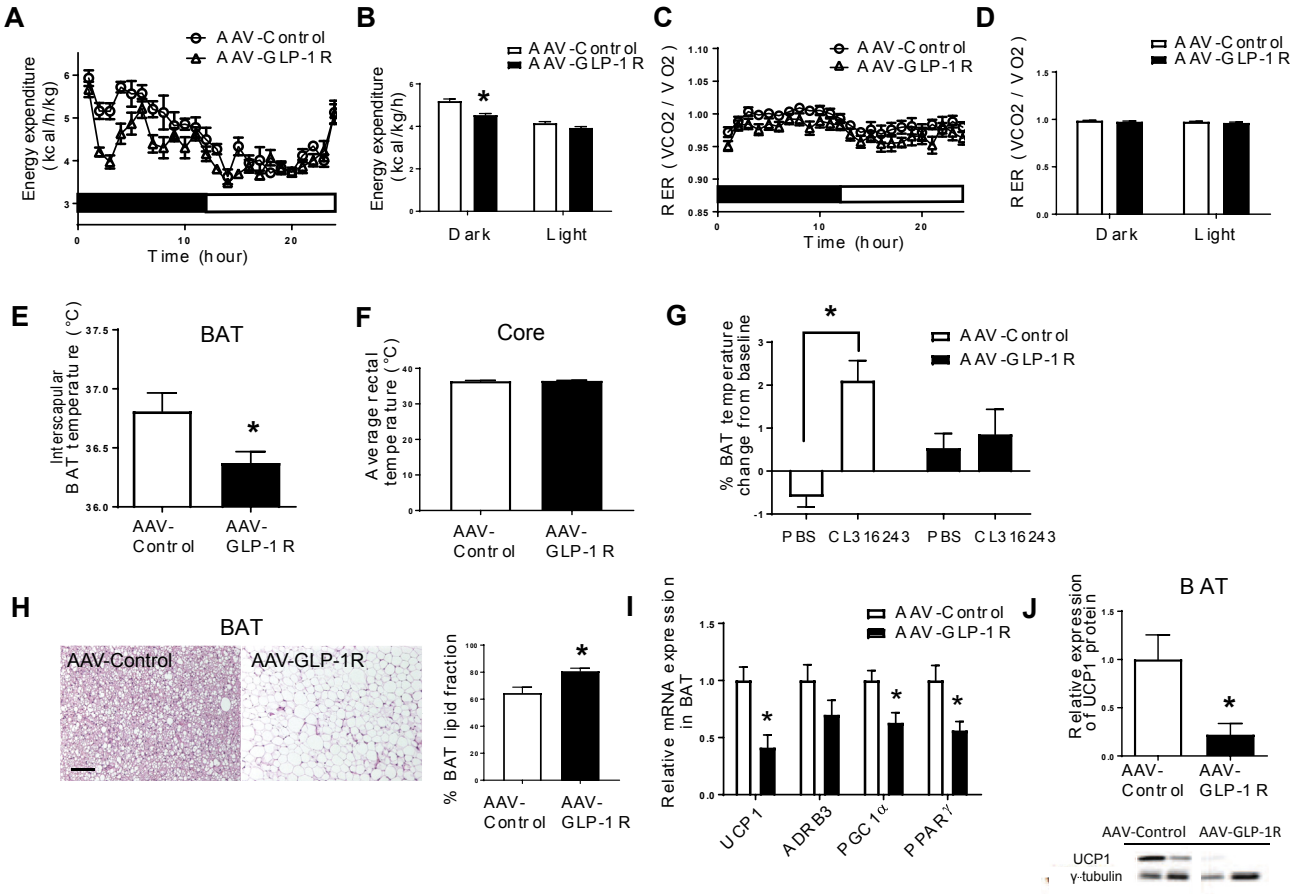

Figure 3: DMH *Glp1r* KD decreases EE and BAT thermogenesis. (A) EE over 24 h in AAV-control and AAV-GLP-1R rats. **(B)** Average EE in dark and light phases (n = 7/9; Two-way ANOVA; *p < 0.0001). **(C)** RER over 24 h in AAV-control and AAV-GLP-1R rats. **(D)** Average RER in dark and light phases. **(E)** BAT temperature during the dark phase (n = 7/8; Student t-test; *p < 0.01). **(F)** Rectal temperature during the dark phase. **(G)** BAT temperate change 2 h after β-3 receptor agonist CL316243 injection (1 μg/kg i.p.; n = 3–5; Two-way ANOVA; *p < 0.005). **(H)** Representative pictures of H&E staining (Scale bar: 100 μm) and lipid area fraction in BAT of AAV-control and AAV-GLP-1R rats (n = 6/5; Student t-test; *p < 0.05). **(I)** Relative mRNA expression of thermogenic markers in BAT: n = 7/8; Student t-test; *p < 0.005 for UCP1; *p < 0.05 for PGC1α, PPARγ. ns: ADRB3. **(J)** Relative UCP1 protein expression in BAT (n = 5/7; Student t-test; *p < 0.01). Data are mean ± SEM.

They were however conspicuously absent from the compact subdivision of DMH (DMHp), which contains the majority of DMH NPY neurons (S4). We found less than 5% of GLP-1R mRNA expressing neurons contained NPY mRNA in the DMH (Figure 5D, S5A), strongly supporting an indirect regulation of NPY by GLP-1R signaling. Numerous GAD65 mRNA-containing neurons were also distributed rostrocaudally in the DMH (S4). We found that a large percentage of GLP-1R mRNA expressing neurons (25–35%) also contained GAD65 mRNA (Figure 5E, S5B). Similarly, NPY neurons in the ARC do not express GLP-1R and the majority of them express GAD65 (Figure 5D,E). A smaller percentage of DMH GLP-1R mRNA neurons (16%) also expressed VGLuT2 mRNA (S5C), indicating that DMH GLP-1R expressing neurons are not exclusively GABAergic. Virtually all NPY mRNA containing neurons, however, were found in the DMHp where there were also substantial numbers of VGluT2 mRNA-containing neurons (S4). Thus, NPY neurons in the DMH are predominantly glutamatergic, whereas DMH GLP-1R-expressing cells are predominantly GABAergic.

3.7. DMH *Glp1r* KD attenuates the anorexigenic effects of peripheral GLP-1R agonist treatment

The anorexigenic effects of peripherally administered agonists are thought to be mediated, in part, by GLP-1R expressing neurons in the brain [8,9,11]. To test whether reduced DMH GLP-1R expression influences the anorexigenic effects of a peripheral GLP-1R agonist, we injected Exendin-4 (Ex-4, 1 μg/kg, IP) and measured BW, food intake, EE and RER. Ex-4 decreased 24 h food intake in the controls (P < 0.01), but this effect was attenuated in AAV-GLP-1R rats (Figure 6A). It is important to mention that the baseline food intake was reduced in AAV-GLP-1R rats after 7 weeks, likely compromising Ex-4's ability to further suppress food intake. Similarly, Ex-4-induced 24 h BW loss was attenuated in AAV-GLP-1R rats compared to the controls (Figure 6B, p < 0.005). In contrast to the stimulatory effects of central GLP-1 or GLP-1 analogs on EE [67,68], peripheral GLP-1/Ex-4 administration decreases RER and diet-induced thermogenesis in rodents and humans [12,69], suggesting that the activation of peripheral or central GLP-1R has opposite effects on EE. Whereas Ex-4 treatment at dark phase onset decreased EE in the controls during dark phase (p < 0.005), it did not further decrease EE in AAV-GLP-1R rats that are in a metabolically compromised state (Figure 6C,D; S6A). Ex-4 treatment also decreased RER in the controls during the dark phase (p < 0.001), but this effect was attenuated in AAV-GLP-1R rats (Figure 6E,F; S6B). Our data demonstrate that DMH GLP-1R expression is necessary for normal EE, and that peripheral Ex-4 treatment fails to decrease food intake and BW in the state of low metabolic efficiency.

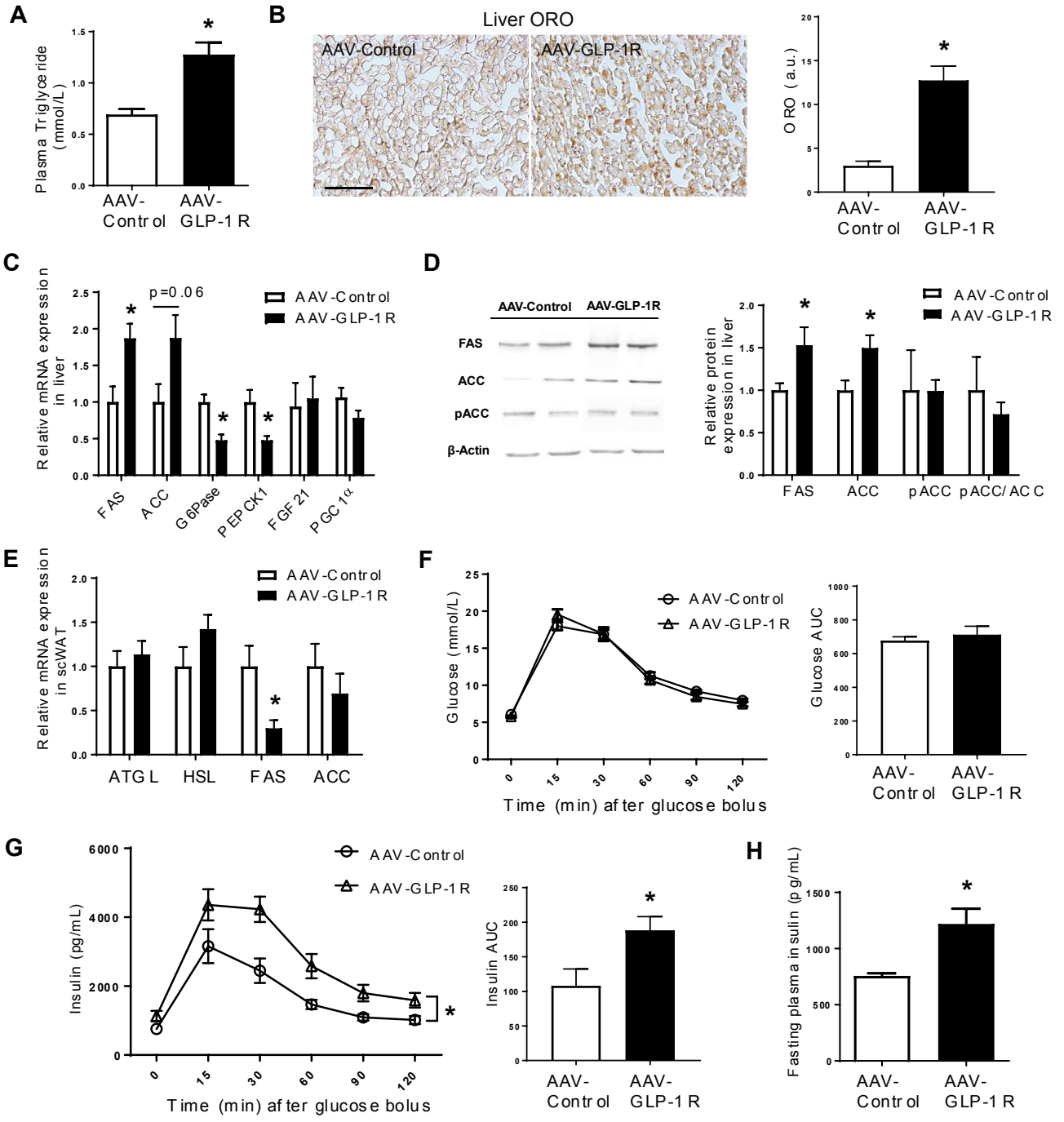

Figure 4: DMH *Glp1r* KD rats develop hepatic steatosis and insulin resistance. (A) Plasma TG levels (n = 6/8; Student t-test; *p < 0.001). **(B)** Representative pictures of oil red O staining (Scale bar: 100 μm) and ORO area quantification in liver of AAV-control and AAV-GLP-1R rats (n = 5/5; Student t-test; p < 0.0005). **(C)** Relative mRNA expression in liver: n = 6/8; Student t-test; *p < 0.05 for FAS * p < 0.01 for PEPCK1; *p < 0.005 for G6Pase. p = 0.06 for ACC, ns: FGF21 and PGC1α. **(D)** Western blot for enzymes involved in do-novo lipogenesis: n = 7/8; Student t-test; *p < 0.05 for FAS and ACC. ns: pACC and pACC/ACC. **(E)** Relative mRNA expression in inguinal fat pad: n = 6/8; Student t-test; *p < 0.05 for FAS. ns: ATGL, HSL, and ACC. **(F)** Blood glucose profile during an IPGTT (2 g/kg glucose) in AAV-control and AAV-GLP-1R rats. The bar graph shows the area under curve. **(G)** Blood insulin profile during an IPGTT in AAV-control and AAV-GLP-1R rats. The bar graph shows the area under curve (n = 4/6; Student t-test; *p < 0.05). **(H)** Fasting plasma insulin levels in AAV-control and AAV-GLP-1R rats (n = 4/6; Student t-test; *p < 0.05). Data are mean ± SEM.

4. DISCUSSION

GLP-1 producing neurons send extensive projections to brain areas involved in the regulation of energy balance [6]. GLP-1 neurons affect food intake and EE primarily by modulating forebrain neural circuitries [16,70–72]. The DMH, a major hypothalamic site receiving GLP-1 projections, is well known for modulating pre-autonomic neurons involved in BAT thermogenesis, HPA-axis activation, and blood pressure [32,73,74]. Here we show that acute GLP-1R stimulation in the DMH increases BAT thermogenesis, whereas viral-mediated *Glp1r* KD in the

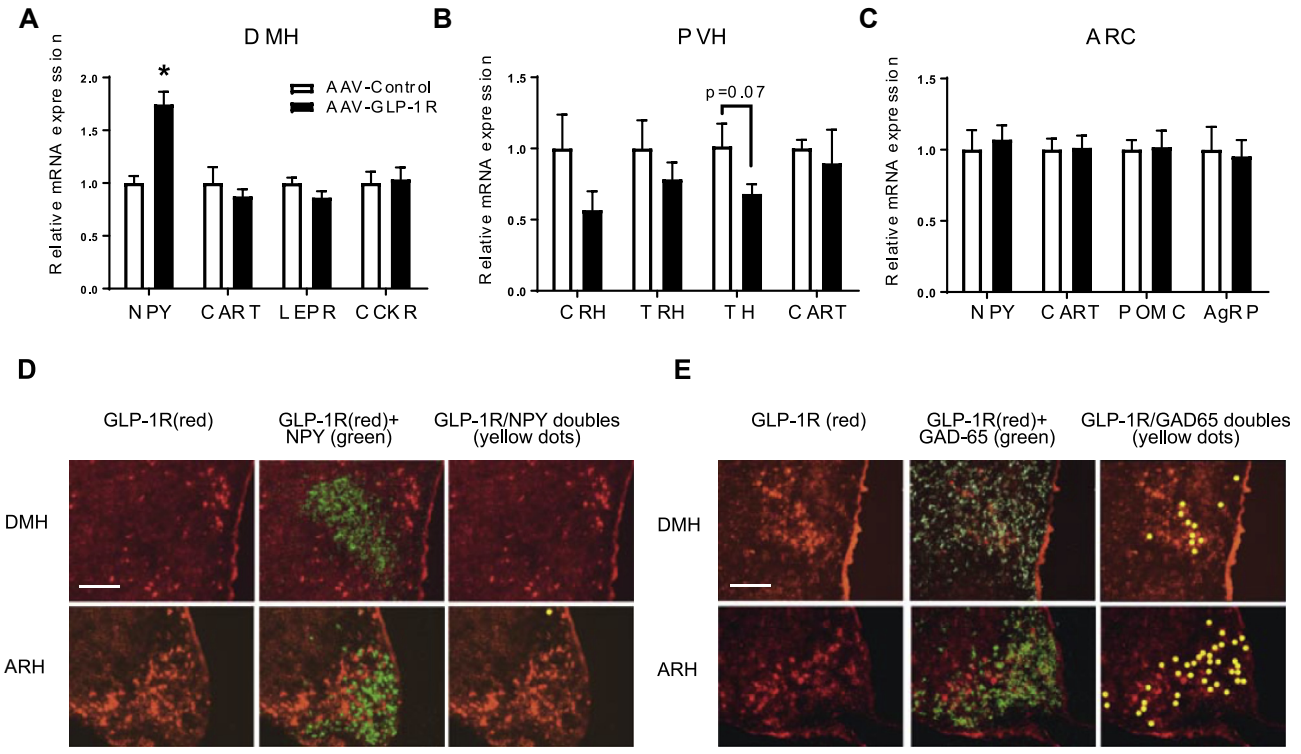

Figure 5: DMH GLP-1R signaling regulates NPY gene expression indirectly. (A) Relative mRNA expression in the DMH in AAV-control and AAV-GLP-1R rats: n = 6/9; Student t-test; *p < 0.0005 for NPY. ns: CART, LEPR, and CCKR. **(B)** Relative mRNA expression in the PVH. ns: CRH, TRH, TH (p = 0.07), and CART. **(C)** Relative mRNA expression in the ARC. ns: NPY, CART, POMC, and AgRP. **(D)** ISH/FISH for GLP-1R and NPY mRNA. Top (DMH) and bottom (ARC) panels: Left-GLP-1R mRNA (red), Middle-GLP-1R (red) and NPY (green), Right-co-localization in yellow. **(E)** ISH/FISH for GLP-1R and GAD-65 mRNA. Top (DMH) and bottom (ARC) panels: Left-GLP-1R mRNA (red), Middle-GLP-1R (red) and GAD-65 (green), Right-co-localization in yellow. Scale bar for all panels = 200 μm. Data are mean ± SEM.

DMH increases adiposity, hepatic steatosis and insulin resistance. In support of obese phenotypes, DMH *Glp1r* KD reduced EE and BAT thermogenesis, with a concomitant increase in DMH NPY mRNA expression. Furthermore, the GLP-1R agonist Ex-4 failed to elicit its full anorexigenic and metabolic effects in DMH *Glp1r* KD rats, raising the possibility that increased NPY in the DMH and low sympathetic tone reduces the efficacy of GLP-1 drug treatment in the obese diabetic state.

A recent report attempted to dissect the role of various hypothalamic GLP-1R expressing neurons by deleting GLP-1R using a cre-lox recombination technology [10]. Surprisingly, their partial knockdown of GLP-1R mRNA in whole hypothalamus, PVH, or specifically in POMC neurons produced inconsistent and very modest effects on BW and EE. Therefore, to avoid developmental compensation of embryonic gene deletion, more time-controlled and region-specific studies targeting different GLP-1R populations in normally-developed adult models are clearly needed. To this end, we used acute pharmacological stimulation and chronic viral-mediated reduction of GLP-1R mRNA in rats to reveal a novel physiological role for GLP-1R signaling effects on DMH neurons known to regulate BAT sympathetic activity.

Central GLP-1R agonism increases EE and BAT thermogenesis [16,18]. In particular, administration of the GLP-1R agonist liraglutide into the ventromedial hypothalamus stimulates BAT thermogenesis and adipocyte browning via hypothalamic AMPK activity [16]. In the same study, DMH GLP-1R stimulation by liraglutide did not alter food intake, BW, or BAT UCP1 expression. In contrast, we demonstrate that native GLP-1 injection into the DMH increases BAT activity and core temperature, as well as BAT thermogenic gene expression. This discrepancy may reflect signaling differences between native GLP-1 and liraglutide, causing differential cellular and behavioral responses. Some evidence suggests that GLP-1 analogs can differentially influence pathway specificity of G-protein coupled receptors [75,76]. Consistent with the effects of acute GLP-1R stimulation, DMH *Glp1r* KD decreased EE, BAT temperature and thermogenic markers. Therefore, it is reasonable to conclude that DMH GLP-1R signaling profoundly affects BAT thermogenesis, presumably by modulating sympathetic nerve activity.

The role of BAT in the regulation of BW is controversial in both humans and animal models [77]. There are many confounding factors including ambient temperature, diet, and body composition, making it difficult to isolate the role of BAT in BW regulation. In fact, UCP1 deficient mice are resistant to obesity unless they are housed in thermoneutrality [78]. Because we housed our animals at a lower temperature, we speculate that the small BW difference developed over several weeks after the KD, and this BW phenotype may be secondary to chronic reduction in BAT function/fuel utilization rather than a direct effect of DMH *Glp1r* KD. Future studies will be necessary to compare the BW effect of DMH *Glp1r* KD in thermoneutrality.

The hypothalamus plays an important role in TG metabolism via sympathetic regulation of BAT, liver, and WAT [15]. Evidence shows that GLP-1 can in part affect TG metabolism via a central mechanism [20,21]. Intriguingly, central GLP-1R agonists increase TG and glucose uptake in the BAT and WAT [18]. Our data show that the DMH is a critical site for GLP-1R-mediated stimulation of BAT thermogenesis, together with hepatic TG production and secretion, which provide additional fuel for BAT heat generation [65]. Central GLP-1R stimulation may also affect hepatic TG production via increased insulin secretion

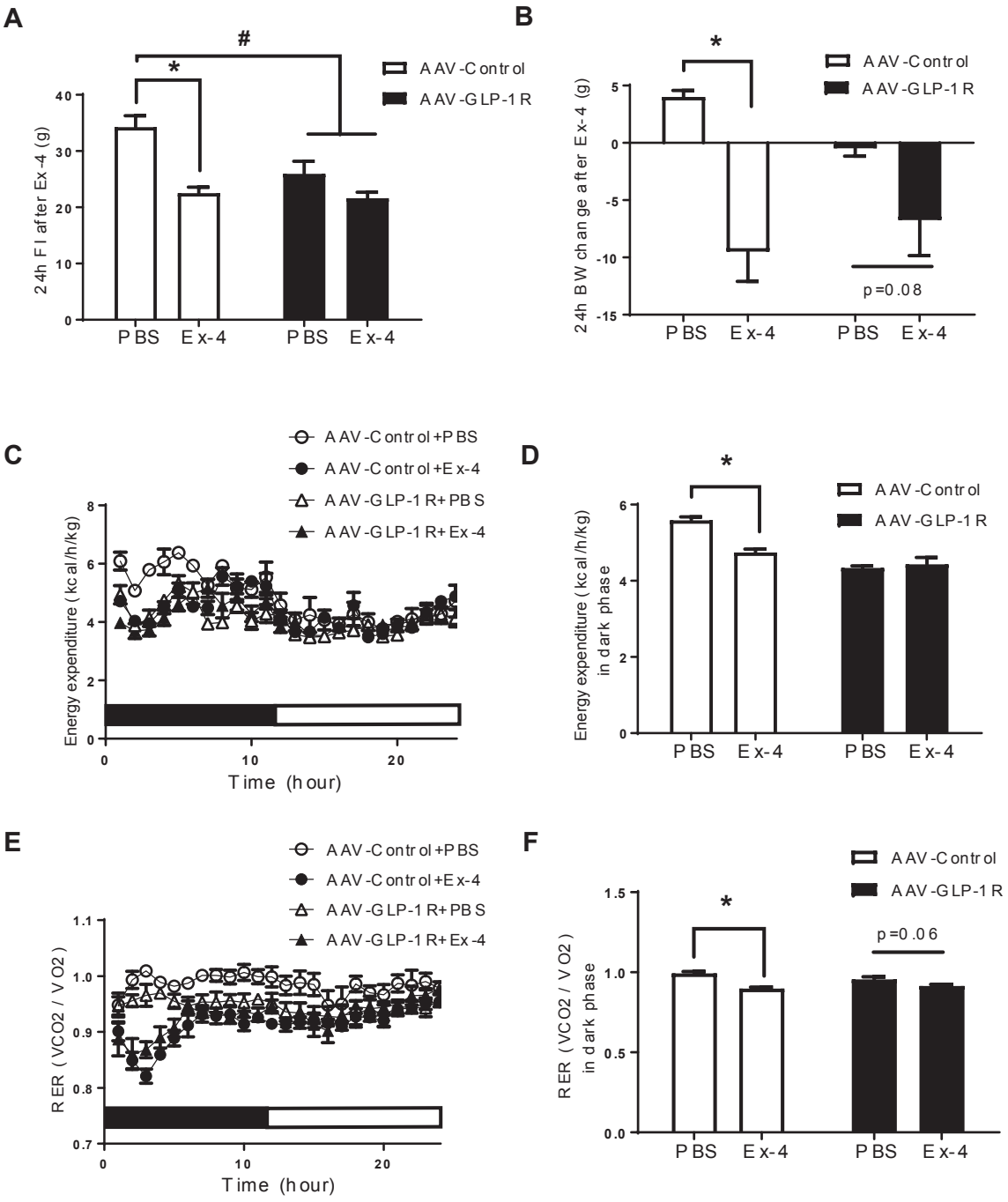

Figure 6: Long term DMH *Glp1r* KD attenuates the anorexigenic response to Ex-4. (A) 24 h food intake after PBS or Ex-4 (1.0 μg/kg, i.p.) treatment in AAV-control and AAV-GLP-1R rats ($n = 7/9$; Two-way ANOVA; drug effect * $p < 0.001$, group effect #$p < 0.05$). **(B)** 24 h BW change after PBS or Ex-4 treatment in AAV-control and AAV-GLP-1R rats ($n = 7/9$; Two-way ANOVA; drug effect * $p < 0.0005$). **(C)** EE over 24 h after PBS or Ex-4 treatment in AAV-control and AAV-GLP-1R rats. **(D)** Average EE in dark phase after PBS or Ex-4 treatment in AAV-control and AAV-GLP-1R rats ($n = 7/9$; Two-way ANOVA; drug effect $p < 0.01$, group effect $p < 0.0001$, *$p < 0.005$). **(E)** RER over 24 h after PBS or Ex-4 treatment in AAV-control and AAV-GLP-1R rats. **(F)** Average RER in dark phase after PBS or Ex-4 treatment in AAV-control and AAV-GLP-1R rats ($n = 7/9$; Two-way ANOVA; drug effect $p < 0.0005$, *$p < 0.001$). Data are mean ± SEM.

[79]. Insulin increases hepatic *de novo* lipogenesis, suppresses fatty acid oxidation, and promotes TG esterification and secretion [80]. We however did not measure plasma insulin after intra DMH GLP-1 injection: therefore, this possibility requires further testing. Intriguingly, long-term DMH *Glp1r* KD also increased hepatic fatty acid synthesis and plasma TG levels, which was associated with increased lipid accumulation in the BAT and hyperinsulinemia. It is widely accepted that defective adaptive thermogenesis contributes to the metabolic syndrome including hepatic steatosis and insulin resistance [81]. Therefore, reduced BAT thermogenesis following long-term DMH *Glp1r* KD likely contributes to the high levels of plasma TG and fat accumulation in the liver.

Recent studies have revealed different DMH neuronal populations linked to BAT thermogenesis [36,44,82–84]. Leptin's thermogenic

effect requires prolactin-releasing peptide neurons in the DMH [82], while cholinergic DMH neurons decrease BAT activity by modulating serotonergic neurons in the rostral raphe pallidus (rRPa) [83]. We now show that DMH NPY mRNA levels are inversely correlated with GLP-1R signaling, which makes NPY a potential downstream substrate for sympathetic regulation of BAT thermogenesis. DMH NPY neurons project to the PVH, where they inhibit the sympathetic drive of BAT [28,85]. More specifically, NPY release in the PVH modulates presynaptic neurotransmitter release and, hence, strongly inhibits the sympathetic stimulation of BAT [86]. Reducing DMH-NPY expression increased UCP1 expression in BAT and promoted the browning of WAT [44]. On the other hand, over-expressing NPY mRNA in the DMH decreased BAT UCP1 expression and caused insulin resistance [87]. Given the role of DMH NPY neurons in BAT thermogenesis, elevated NPY is well placed to be a key contributor to the low BAT activity seen in DMH *Glp1r* KD rats.

Another recent study demonstrated that DMH NPY mRNA knockdown suppresses hepatic glucose production and increases insulin sensitivity via hepatic vagal innervation [45]. Our data also support the role of DMH NPY expression in hepatic glucose metabolism. DMH NPY overexpression induced by *Glp1r* KD was associated with the development of hepatic steatosis and whole body insulin resistance. However, PEPCK and G6Pase gene expression was down-regulated in our DMH *Glp1r* KD model, suggesting a differential mechanism contributing to insulin resistance. Although we cannot rule out the possibility that *Glp1r* KD directly affected hepatic glucose metabolism via an NPY-dependent pathway, defective BAT function may be the primary underlying cause of energy imbalance and insulin resistance as its normal function is important for the clearance of glucose and triglycerides from the circulation [88,89]. Further studies using BAT or hepatic sympathetic denervation techniques are necessary to implicate the role of DMH GLP-1R signaling in hepatic glucose and lipid metabolism.

The mechanism by which DMH GLP-1R signaling regulates NPY expression in the DMH remains unclear. Previous studies have shown that peripheral Ex-4 treatment decreases ARC NPY expression [90,91]. Moreover, GLP-1 treatment inhibited the electrical activity of ARC NPY neurons, which required GABAergic presynaptic input [9]. This is further supported by our observation that GLP-1R mRNA is not found in ARC NPY neurons, and by the lack of labeled GLP-1 uptake by NPY neurons in the ARC [9]. Although ARC and DMH NPY expression is differentially regulated by fasting and diet-induced obesity [92,93], a similar mechanism may play a role in regulating NPY expression in the DMH. Indeed, using two ISH techniques, we unequivocally demonstrate that DMH GLP-1R neurons do not express NPY, which means that GLP-1R signaling must regulate NPY expression indirectly. The fact that many DMH GLP-1R neurons are GABAergic supports a local inhibitory mechanism used by GLP-1 signaling to suppress NPY expression. However, based on anatomical evidence, we cannot exclude the possibility that a combined action of GABAergic and glutamatergic GLP-1R expressing neurons in the DMH modulates NPY expression and consequently sympathetic output to BAT by way of the PVH or the rRPa. Further studies are needed to dissect the DMH GLP-1R signaling influences on the neural substrates and pathways that lead to BAT thermogenesis. Finally, we note that our methods were not designed to account for all possible chemical phenotypes that express GLP-1R mRNA. Other studies have shown that DMH neurons express a range of neuropeptides and metabolically important receptors, including the leptin receptor [36], orexin [94], CART [95], and prolactin—releasing peptide [82]. This means that GLP-1R mRNA is found in a diverse but as yet uncharacterized set of DMH neurons.

Liraglutide, a GLP-1R agonist, has recently been approved for obesity treatment [96], and the mechanisms of its anorexigenic effects are still under active investigation. Because central GLP-1R expressing neurons are the key mediators for the anorexigenic effects of peripheral GLP-1R agonists [8,9,11], reduced hypothalamic GLP-1R expression and activity could explain the decreased sensitivity to GLP-1R agonists seen in obese diabetic conditions [97,98]. While ARC GLP-1R expressing cells are thought to mediate the anorexigenic effects of liraglutide [9], bilateral GLP-1 infusion into the ARC did not affect food intake [99]. Moreover, a study employing a POMC specific GLP-1R KO showed normal BW and food intake phenotypes during standard chow feeding [10]. Therefore, the exact role of ARC GLP-1R in food intake is still unclear. Our data showed that altered DMH GLP-1R expression does not affect daily food intake and the reduced refeeding response to overnight fasting presumably reflects a lower metabolic efficiency due to compromised BAT function. Therefore, our *Glp1r* KD model provides a valuable tool for understanding the clinical significance of reduced DMH GLP-1R signaling that appears to be critical for BAT regulation. BAT depots are present in adult humans where their thermogenic properties are metabolically beneficial [100,101]. Based on our findings following DMH *Glp1r* KD in rats, the attenuated anorexigenic response to peripheral Ex-4 treatment is correlated with reduced BAT thermogenic capacity. This means that obese diabetic patients with reduced BAT function may exhibit a central GLP-1 resistance that limits the effectiveness of GLP-1R agonist treatment as a weight loss strategy, although this hypothesis requires further testing.

5. CONCLUSIONS

Central GLP-1 relays peripheral nutrient and hormonal signals to the hypothalamus and other energy balance-relevant nuclei distributed across the neuraxis [3,6,25]. It is therefore imperative to clarify how hypothalamic GLP-1R signaling regulates energy balance and how its impairment contributes to the pathophysiology of metabolic syndrome and the efficacy of GLP-1 therapy. Our results point to an important link between hindbrain GLP-1 projections into the DMH and NPY-mediated sympathetic regulation of BAT thermogenesis and energy balance. In light of our findings, manipulating central GLP-1 production and receptor activation in a site-specific manner may hold the key to developing future therapeutic strategies for metabolic syndrome.

ACKNOWLEDGEMENTS

We thank Emily Nobel (Scott E. Kanoski lab, University of Southern California) for her help during RNA scope experiment. We also thank our ETH laboratory members, especially Rosmarie Clara for her help during the experiments.

This work was supported by SNSF MHV grant PMPDP3_151360 (S.J. Lee), ETH Research Grant 47 12-2 (W. Langhans and S.J. Lee), SNSF ISV grant IZK0Z3 173687 (S.J. Lee and A.G. Watts), SNSF ISV grant IZK0Z3 158027 (A.G. Watts and W. Langhans), NS029728 (A.G. Watts), NIH-DK096139 (M.R. Hayes), DK104897 (S.E. Kanoski).

Conceptualization, S.J. Lee, A.G. Watts, and W. Langhans.; Investigation, S.J. Lee, G.S. Watts, A. Cortell, A. Pignalosa, J-P. Krieger, K.G. Pettersen, P.N. Norell, Dubravka Vrdoljak; Writing S.J.L; Review & editing, S.J. Lee, M.R. Hayes, S.E. Kanoski, A.G. Watts, and W. Langhans.; S.J. Lee is the guarantor of the work and takes full responsibility for the integrity of data and the accuracy of data analyses.

CONFLICT OF INTEREST

None declared.

APPENDIX A. SUPPLEMENTARY DATA

Supplementary data related to this article can be found at https://doi.org/10.1016/j.molmet.2018.03.008.

REFERENCES

[1] Drucker, D.J., 1998. Glucagon-like peptides. Diabetes 47:159–169.

[2] Holst, J.J., 1994. Glucagonlike peptide 1: a newly discovered gastrointestinal hormone. Gastroenterology 107:1848–1855.

[3] Trapp, S., Richards, J.E., 2013. The gut hormone glucagon-like peptide-1 produced in brain: is this physiologically relevant? Current Opinion in Pharmacology 13:964–969.

[4] Cork, S.C., Richards, J.E., Holt, M.K., Gribble, F.M., Reimann, F., Trapp, S., 2015. Distribution and characterisation of Glucagon-like peptide-1 receptor expressing cells in the mouse brain. Molecular Metabolism 4:718–731.

[5] Gu, G., Roland, B., Tomaselli, K., Dolman, C.S., Lowe, C., Heilig, J.S., 2013. Glucagon-like peptide-1 in the rat brain: distribution of expression and functional implication. The Journal of Comparative Neurology 521:2235–2261.

[6] Llewellyn-Smith, I.J., Reimann, F., Gribble, F.M., Trapp, S., 2011. Preproglucagon neurons project widely to autonomic control areas in the mouse brain. Neuroscience 180:111–121.

[7] Rajeev, S.P., Wilding, J., 2016. GLP-1 as a target for therapeutic intervention. Current Opinion in Pharmacology 31:44–49.

[8] Sisley, S., Gutierrez-Aguilar, R., Scott, M., D'Alessio, D.A., Sandoval, D.A., Seeley, R.J., 2014. Neuronal GLP1R mediates liraglutide's anorectic but not glucose-lowering effect. Journal of Clinical Investigation 124:2456–2463.

[9] Secher, A., Jelsing, J., Baquero, A.F., Hecksher-Sorensen, J., Cowley, M.A., Dalboge, L.S., et al., 2014. The arcuate nucleus mediates GLP-1 receptor agonist liraglutide-dependent weight loss. Journal of Clinical Investigation 124:4473–4488.

[10] Burmeister, M.A., Ayala, J.E., Smouse, H., Landivar-Rocha, A., Brown, J.D., Drucker, D.J., et al., 2017 Feb. The hypothalamic glucagon-like Peptide-1 (GLP-1) receptor (GLP-1R) is sufficient but not necessary for the regulation of energy balance and glucose homeostasis in mice. Diabetes 66(2):372–384.

[11] Kanoski, S.E., Fortin, S.M., Arnold, M., Grill, H.J., Hayes, M.R., 2011. Peripheral and central GLP-1 receptor populations mediate the anorectic effects of peripherally administered GLP-1 receptor agonists, liraglutide and exendin-4. Endocrinology 152:3103–3112.

[12] Baggio, L.L., Huang, Q., Brown, T.J., Drucker, D.J., 2004. Oxyntomodulin and glucagon-like peptide-1 differentially regulate murine food intake and energy expenditure. Gastroenterology 127:546–558.

[13] Hwa, J.J., Ghibaudi, L., Williams, P., Witten, M.B., Tedesco, R., Strader, C.D., 1998. Differential effects of intracerebroventricular glucagon-like peptide-1 on feeding and energy expenditure regulation. Peptides 19:869–875.

[14] Lockie, S.H., Heppner, K.M., Chaudhary, N., Chabenne, J.R., Morgan, D.A., Veyrat-Durebex, C., et al., 2012. Direct control of brown adipose tissue thermogenesis by central nervous system glucagon-like peptide-1 receptor signaling. Diabetes 61:2753–2762.

[15] Geerling, J.J., Boon, M.R., Kooijman, S., Parlevliet, E.T., Havekes, L.M., Romijn, J.A., et al., 2014. Sympathetic nervous system control of triglyceride metabolism: novel concepts derived from recent studies. The Journal of Lipid Research 55:180–189.

[16] Beiroa, D., Imbernon, M., Gallego, R., Senra, A., Herranz, D., Villarroya, F., et al., 2014. GLP-1 agonism stimulates brown adipose tissue thermogenesis and browning through hypothalamic AMPK. Diabetes 63:3346–3358.

[17] Heppner, K.M., Marks, S., Holland, J., Ottaway, N., Smiley, D., Dimarchi, R., et al., 2015. Contribution of brown adipose tissue activity to the control of energy balance by GLP-1 receptor signalling in mice. Diabetologia 58:2124–2132.

[18] Kooijman, S., Wang, Y., Parlevliet, E.T., Boon, M.R., Edelschaap, D., Snaterse, G., et al., 2015. Central GLP-1 receptor signalling accelerates plasma clearance of triacylglycerol and glucose by activating brown adipose tissue in mice. Diabetologia 58:2637–2646.

[19] Wei, Q., Li, L., Chen, J.A., Wang, S.H., Sun, Z.L., 2015. Exendin-4 improves thermogenic capacity by regulating fat metabolism on brown adipose tissue in mice with diet-induced obesity. Annals of Clinical and Laboratory Science 45:158–165.

[20] Nogueiras, R., Perez-Tilve, D., Veyrat-Durebex, C., Morgan, D.A., Varela, L., Haynes, W.G., et al., 2009. Direct control of peripheral lipid deposition by CNS GLP-1 receptor signaling is mediated by the sympathetic nervous system and blunted in diet-induced obesity. Journal of Neuroscience: The Official Journal of the Society for Neuroscience 29:5916–5925.

[21] Panjwani, N., Mulvihill, E.E., Longuet, C., Yusta, B., Campbell, J.E., Brown, T.J., et al., 2013. GLP-1 receptor activation indirectly reduces hepatic lipid accumulation but does not attenuate development of atherosclerosis in diabetic male ApoE(-/-) mice. Endocrinology 154:127–139.

[22] Ten Kulve, J.S., van Bloemendaal, L., Balesar, R., IJzerman, R.G., Swaab, D.F., Diamant, M., et al., 2016. Decreased hypothalamic glucagon-like Peptide-1 receptor expression in type 2 diabetes patients. Journal of Clinical Endocrinology & Metabolism 101:2122–2129.

[23] Morrison, S.F., Madden, C.J., Tupone, D., 2012. Central control of brown adipose tissue thermogenesis. Frontiers in Endocrinology 3.

[24] Renner, E., Puskas, N., Dobolyi, A., Palkovits, M., 2012. Glucagon-like peptide-1 of brainstem origin activates dorsomedial hypothalamic neurons in satiated rats. Peptides 35:14–22.

[25] Trapp, S., Cork, S.C., 2015. PPG neurons of the lower brain stem and their role in brain GLP-1 receptor activation. American Journal of Physiology - Regulatory, Integrative and Comparative Physiology 309:R795–R804.

[26] Bamshad, M., Song, C.K., Bartness, T.J., 1999. CNS origins of the sympathetic nervous system outflow to brown adipose tissue. American Journal of Physiology 276:R1569–R1578.

[27] Cano, G., Passerin, A.M., Schiltz, J.C., Card, J.P., Morrison, S.F., Sved, A.F., 2003. Anatomical substrates for the central control of sympathetic outflow to interscapular adipose tissue during cold exposure. The Journal of Comparative Neurology 460:303–326.

[28] Lee, S.J., Kirigiti, M., Lindsley, S.R., Loche, A., Madden, C.J., Morrison, S.F., et al., 2013. Efferent projections of neuropeptide Y-expressing neurons of the dorsomedial hypothalamus in chronic hyperphagic models. The Journal of Comparative Neurology 521:1891–1914.

[29] Oldfield, B.J., Giles, M.E., Watson, A., Anderson, C., Colvill, L.M., McKinley, M.J., 2002. The neurochemical characterisation of hypothalamic pathways projecting polysynaptically to brown adipose tissue in the rat. Neuroscience 110:515–526.

[30] Cao, W.H., Fan, W., Morrison, S.F., 2004. Medullary pathways mediating specific sympathetic responses to activation of dorsomedial hypothalamus. Neuroscience 126:229–240.

[31] Zaretskaia, M.V., Zaretsky, D.V., Shekhar, A., DiMicco, J.A., 2002. Chemical stimulation of the dorsomedial hypothalamus evokes non-shivering thermogenesis in anesthetized rats. Brain Research 928:113–125.

[32] Ulrich-Lai, Y.M., Herman, J.P., 2009. Neural regulation of endocrine and autonomic stress responses. Nature Reviews Neuroscience 10:397–409.

[33] Simonds, S.E., Pryor, J.T., Ravussin, E., Greenway, F.L., Dileone, R., Allen, A.M., et al., 2014. Leptin mediates the increase in blood pressure associated with obesity. Cell 159:1404–1416.

[34] Enriori, P.J., Sinnayah, P., Simonds, S.E., Garcia Rudaz, C., Cowley, M.A., 2011. Leptin action in the dorsomedial hypothalamus increases sympathetic tone to brown adipose tissue in spite of systemic leptin resistance. Journal of Neuroscience: The Official Journal of the Society for Neuroscience 31:12189–12197.

[35] Rezai-Zadeh, K., Yu, S., Jiang, Y., Laque, A., Schwartzenburg, C., Morrison, C.D., et al., 2014. Leptin receptor neurons in the dorsomedial hypothalamus are key regulators of energy expenditure and body weight, but not food intake. Molecular Metabolism 3:681–693.

[36] Zhang, Y., Kerman, I.A., Laque, A., Nguyen, P., Faouzi, M., Louis, G.W., et al., 2011. Leptin-receptor-expressing neurons in the dorsomedial hypothalamus and median preoptic area regulate sympathetic brown adipose tissue circuits. Journal of Neuroscience: The Official Journal of the Society for Neuroscience 31:1873–1884.

[37] Elmquist, J.K., Bjorbaek, C., Ahima, R.S., Flier, J.S., Saper, C.B., 1998. Distributions of leptin receptor mRNA isoforms in the rat brain. The Journal of Comparative Neurology 395:535–547.

[38] Merchenthaler, I., Lane, M., Shughrue, P., 1999. Distribution of pre-pro-glucagon and glucagon-like peptide-1 receptor messenger RNAs in the rat central nervous system. The Journal of Comparative Neurology 403:261–280.

[39] Bellinger, L.L., Bernardis, L.L., 2002. The dorsomedial hypothalamic nucleus and its role in ingestive behavior and body weight regulation: lessons learned from lesioning studies. Physiology & Behavior 76:431–442.

[40] Grove, K.L., Brogan, R.S., Smith, M.S., 2001. Novel expression of neuropeptide Y (NPY) mRNA in hypothalamic regions during development: region-specific effects of maternal deprivation on NPY and Agouti-related protein mRNA. Endocrinology 142:4771–4776.

[41] Guan, X.M., Yu, H., Trumbauer, M., Frazier, E., Van der Ploeg, L.H., Chen, H., 1998. Induction of neuropeptide Y expression in dorsomedial hypothalamus of diet-induced obese mice. NeuroReport 9:3415–3419.

[42] Kesterson, R.A., Huszar, D., Lynch, C.A., Simerly, R.B., Cone, R.D., 1997. Induction of neuropeptide Y gene expression in the dorsal medial hypothalamic nucleus in two models of the agouti obesity syndrome. Molecular Endocrinology 11:630–637.

[43] Li, C., Chen, P., Smith, M.S., 1998. Neuropeptide Y (NPY) neurons in the arcuate nucleus (ARH) and dorsomedial nucleus (DMH), areas activated during lactation, project to the paraventricular nucleus of the hypothalamus (PVH). Regulatory Peptides 75–76:93–100.

[44] Chao, P.T., Yang, L., Aja, S., Moran, T.H., Bi, S., 2011. Knockdown of NPY expression in the dorsomedial hypothalamus promotes development of brown adipocytes and prevents diet-induced obesity. Cell Metabolism 13:573–583.

[45] Li, L., de La Serre, C.B., Zhang, N., Yang, L., Li, H., Bi, S., 2016. Knockdown of neuropeptide Y in the dorsomedial hypothalamus promotes hepatic insulin sensitivity in male rats. Endocrinology en20161662.

[46] Kim, Y.J., Bi, S., 2016. Knockdown of neuropeptide Y in the dorsomedial hypothalamus reverses high-fat diet-induced obesity and impaired glucose tolerance in rats. American Journal of Physiology - Regulatory, Integrative and Comparative Physiology 310:R134–R142.

[47] Bartness, T.J., 2011. A potential link between dorsomedial hypothalamic nucleus NPY and energy balance. Cell Metabolism 13:493–494.

[48] Schmidt, H.D., Mietlicki-Baase, E.G., Ige, K.Y., Maurer, J.J., Reiner, D.J., Zimmer, D.J., et al., 2016 Jun. Glucagon-Like Peptide-1 receptor activation in the ventral tegmental area decreases the reinforcing efficacy of cocaine. Neuropsychopharmacology: Official Publication of the American College of Neuropsychopharmacology 41(7):1917–1928.

[49] Alhadeff, A.L., Mergler, B.D., Zimmer, D.J., Turner, C.A., Reiner, D.J., Schmidt, H.D., et al., 2017 Jun. Endogenous glucagon-like Peptide-1 receptor signaling in the nucleus tractus solitarius is required for food intake control. Neuropsychopharmacology: Official Publication of the American College of Neuropsychopharmacology 42(7):1471–1479.

[50] Even, P.C., Nadkarni, N.A., 2012. Indirect calorimetry in laboratory mice and rats: principles, practical considerations, interpretation and perspectives. American Journal of Physiology–Regulatory, Integrative and Comparative Physiology 303:R459–R476.

[51] Tschop, M.H., Speakman, J.R., Arch, J.R., Auwerx, J., Bruning, J.C., Chan, L., et al., 2011. A guide to analysis of mouse energy metabolism. Nature Methods 9:57–63.

[52] Ruttimann, E.B., Arnold, M., Hillebrand, J.J., Geary, N., Langhans, W., 2009. Intrameal hepatic portal and intraperitoneal infusions of glucagon-like peptide-1 reduce spontaneous meal size in the rat via different mechanisms. Endocrinology 150:1174–1181.

[53] Hillebrand, J.J., Langhans, W., Geary, N., 2010. Validation of computed tomographic estimates of intra-abdominal and subcutaneous adipose tissue in rats and mice. Obesity (Silver Spring) 18:848–853.

[54] Mehlem, A., Hagberg, C.E., Muhl, L., Eriksson, U., Falkevall, A., 2013. Imaging of neutral lipids by oil red O for analyzing the metabolic status in health and disease. Nature Protocols 8:1149–1154.

[55] Langhans, W., 1991. Hepatic and intestinal handling of metabolites during feeding in rats. Physiology & Behavior 49:1203–1209.

[56] Schober, G., Arnold, M., Birtles, S., Buckett, L.K., Pacheco-Lopez, G., Turnbull, A.V., et al., 2013. Diacylglycerol acyltransferase-1 inhibition enhances intestinal fatty acid oxidation and reduces energy intake in rats. The Journal of Lipid Research 54:1369–1384.

[57] Watts, A.G., Sanchez-Watts, G., 1995. Physiological regulation of peptide messenger RNA colocalization in rat hypothalamic paraventricular medial parvicellular neurons. The Journal of Comparative Neurology 352:501–514.

[58] Swanson, L.W., 2004. Brain maps: structure of the rat brain. A laboratory guide with printed and electronic templates for data, models and schematics., 3rd revised edition. Amsterdam: Elsevier.

[59] Watts, A.G., Sanchez-Watts, G., 2007. Rapid and preferential activation of Fos protein in hypocretin/orexin neurons following the reversal of dehydration-anorexia. The Journal of Comparative Neurology 502:768–782.

[60] Hsu, T.M., Noble, E.E., Liu, C.M., Cortella, A.M., Konanur, V.R., Suarez, A.N., et al., 2017. A hippocampus to prefrontal cortex neural pathway inhibits food motivation through glucagon-like peptide-1 signaling. Molecular Psychiatry. https://doi.org/10.1038/mp.2017.91 [Advance online publication].

[61] Ziegler, D.R., Cullinan, W.E., Herman, J.P., 2002. Distribution of vesicular glutamate transporter mRNA in rat hypothalamus. The Journal of Comparative Neurology 448:217–229.

[62] Esclapez, M., Tillakaratne, N.J., Tobin, A.J., Houser, C.R., 1993. Comparative localization of mRNAs encoding two forms of glutamic acid decarboxylase with nonradioactive in situ hybridization methods. The Journal of Comparative Neurology 331:339–362.

[63] Watts, A.G., Sanchez-Watts, G., Kelly, A.B., 1999. Distinct patterns of neuropeptide gene expression in the lateral hypothalamic area and arcuate nucleus are associated with dehydration-induced anorexia. Journal of Neuroscience: The Official Journal of the Society for Neuroscience 19:6111–6121.

[64] Yamamoto, H., Kishi, T., Lee, C.E., Choi, B.J., Fang, H., Hollenberg, A.N., et al., 2003. Glucagon-like peptide-1-responsive catecholamine neurons in the area postrema link peripheral glucagon-like peptide-1 with central autonomic control sites. Journal of Neuroscience: The Official Journal of the Society for Neuroscience 23:2939–2946.

[65] Townsend, K.L., Tseng, Y.H., 2014. Brown fat fuel utilization and thermogenesis. Trends in Endocrinology and Metabolism 25:168–177.

[66] Shi, Y.C., Lau, J., Lin, Z., Zhang, H., Zhai, L., Sperk, G., et al., 2013. Arcuate NPY controls sympathetic output and BAT function via a relay of tyrosine hydroxylase neurons in the PVN. Cell Metabolism 17:236–248.

[67] Osaka, T., Endo, M., Yamakawa, M., Inoue, S., 2005. Energy expenditure by intravenous administration of glucagon-like peptide-1 mediated by the lower brainstem and sympathoadrenal system. Peptides 26:1623–1631.

[68] Shalev, A., Holst, J.J., Keller, U., 1997. Effects of glucagon-like peptide 1 (7-36 amide) on whole-body protein metabolism in healthy man. European Journal of Clinical Investigation 27:10–16.

[69] Flint, A., Raben, A., Rehfeld, J.F., Holst, J.J., Astrup, A., 2000. The effect of glucagon-like peptide-1 on energy expenditure and substrate metabolism in humans. International Journal of Obesity and Related Metabolic Disorders 24: 288–298.

[70] Mietlicki-Baase, E.G., Ortinski, P.I., Reiner, D.J., Sinon, C.G., McCutcheon, J.E., Pierce, R.C., et al., 2014. Glucagon-like peptide-1 receptor activation in the nucleus accumbens core suppresses feeding by increasing glutamatergic AMPA/kainate signaling. Journal of Neuroscience: The Official Journal of the Society for Neuroscience 34:6985–6992.

[71] Dossat, A.M., Diaz, R., Gallo, L., Panagos, A., Kay, K., Williams, D.L., 2013. Nucleus accumbens GLP-1 receptors influence meal size and palatability. American Journal of Physiology. Endocrinology and Metabolism 304:E1314–E1320.

[72] Skibicka, K.P., 2013. The central GLP-1: implications for food and drug reward. Frontiers in Neuroscience 7:181.

[73] Morrison, S.F., Madden, C.J., Tupone, D., 2014. Central neural regulation of brown adipose tissue thermogenesis and energy expenditure. Cell Metabolism 19:741–756.

[74] Dampney, R.A., Coleman, M.J., Fontes, M.A., Hirooka, Y., Horiuchi, J., Li, Y.W., et al., 2002. Central mechanisms underlying short- and long-term regulation of the cardiovascular system. Clinical and Experimental Pharmacology and Physiology 29:261–268.

[75] Weston, C., Lu, J., Li, N., Barkan, K., Richards, G.O., Roberts, D.J., et al., 2015. Modulation of glucagon receptor pharmacology by receptor activity-modifying Protein-2 (RAMP2). Journal of Biological Chemistry 290:23009–23022.

[76] Weston, C., Poyner, D., Patel, V., Dowell, S., Ladds, G., 2014. Investigating G protein signalling bias at the glucagon-like peptide-1 receptor in yeast. British journal of pharmacology 171:3651–3665.

[77] Ravussin, E., Galgani, J.E., 2011. The implication of brown adipose tissue for humans. Annual Review of Nutrition 31:33–47.

[78] Liu, X., Rossmeisl, M., McClaine, J., Riachi, M., Harper, M.E., Kozak, L.P., 2003. Paradoxical resistance to diet-induced obesity in UCP1-deficient mice. Journal of Clinical Investigation 111:399–407.

[79] Knauf, C., Cani, P.D., Perrin, C., Iglesias, M.A., Maury, J.F., Bernard, E., et al., 2005. Brain glucagon-like peptide-1 increases insulin secretion and muscle insulin resistance to favor hepatic glycogen storage. Journal of Clinical Investigation 115:3554–3563.

[80] Titchenell, P.M., Lazar, M.A., Birnbaum, M.J., 2017. Unraveling the regulation of hepatic metabolism by insulin. Trends in Endocrinology and Metabolism 28:497–505.

[81] Poekes, L., Legry, V., Schakman, O., Detrembleur, C., Bol, A., Horsmans, Y., et al., 2017. Defective adaptive thermogenesis contributes to metabolic syndrome and liver steatosis in obese mice. Clinical Science(London) 131: 285–296.

[82] Dodd, G.T., Worth, A.A., Nunn, N., Korpal, A.K., Bechtold, D.A., Allison, M.B., et al., 2014. The thermogenic effect of leptin is dependent on a distinct population of prolactin-releasing peptide neurons in the dorsomedial hypothalamus. Cell Metabolism 20:639–649.

[83] Jeong, J.H., Lee, D.K., Blouet, C., Ruiz, H.H., Buettner, C., Chua Jr., S., et al., 2015. Cholinergic neurons in the dorsomedial hypothalamus regulate mouse brown adipose tissue metabolism. Molecular Metabolism 4:483–492.

[84] Kataoka, N., Hioki, H., Kaneko, T., Nakamura, K., 2014. Psychological stress activates a dorsomedial hypothalamus-medullary raphe circuit driving brown adipose tissue thermogenesis and hyperthermia. Cell Metabolism 20:346–358.

[85] Madden, C.J., Morrison, S.F., 2009. Neurons in the paraventricular nucleus of the hypothalamus inhibit sympathetic outflow to brown adipose tissue. American Journal of Physiology - Regulatory, Integrative and Comparative Physiology 296:R831–R843.

[86] Egawa, M., Yoshimatsu, H., Bray, G.A., 1991. Neuropeptide Y suppresses sympathetic activity to interscapular brown adipose tissue in rats. American Journal of Physiology 260:R328–R334.

[87] Zheng, F., Kim, Y.J., Chao, P.T., Bi, S., 2013. Overexpression of neuropeptide Y in the dorsomedial hypothalamus causes hyperphagia and obesity in rats. Obesity 21:1086–1092.

[88] Bartelt, A., Bruns, O.T., Reimer, R., Hohenberg, H., Ittrich, H., Peldschus, K., et al., 2011. Brown adipose tissue activity controls triglyceride clearance. Nature Medicine 17:200–205.

[89] Stanford, K.I., Middelbeek, R.J., Townsend, K.L., An, D., Nygaard, E.B., Hitchcox, K.M., et al., 2013. Brown adipose tissue regulates glucose homeostasis and insulin sensitivity. Journal of Clinical Investigation 123:215–223.

[90] Lee, S.J., Diener, K., Kaufman, S., Krieger, J.P., Pettersen, K.G., Jejelava, N., et al., 2016. Limiting glucocorticoid secretion increases the anorexigenic property of Exendin-4. Molecular Metabolism 5:552–565.

[91] Yang, Y., Moghadam, A.A., Cordner, Z.A., Liang, N.C., Moran, T.H., 2014. Long term exendin-4 treatment reduces food intake and body weight and alters expression of brain homeostatic and reward markers. Endocrinology 155:3473–3483.

[92] Bi, S., Kim, Y.J., Zheng, F., 2012. Dorsomedial hypothalamic NPY and energy balance control. Neuropeptides 46:309–314.

[93] Draper, S., Kirigiti, M., Glavas, M., Grayson, B., Chong, C.N., Jiang, B., et al., 2010. Differential gene expression between neuropeptide Y expressing neurons of the dorsomedial nucleus of the hypothalamus and the arcuate nucleus: microarray analysis study. Brain Research 1350:139–150.

[94] Swanson, L.W., Sanchez-Watts, G., Watts, A.G., 2005. Comparison of melanin-concentrating hormone and hypocretin/orexin mRNA expression patterns in a new parceling scheme of the lateral hypothalamic zone. Neuroscience Letters 387:80–84.

[95] Lee, S.J., Verma, S., Simonds, S.E., Kirigiti, M.A., Kievit, P., Lindsley, S.R., et al., 2013. Leptin stimulates neuropeptide Y and cocaine amphetamine-regulated transcript coexpressing neuronal activity in the dorsomedial hypothalamus in diet-induced obese mice. Journal of Neuroscience: The Official Journal of the Society for Neuroscience 33:15306–15317.

[96] Pi-Sunyer, X., Astrup, A., Fujioka, K., Greenway, F., Halpern, A., Krempf, M., et al., 2015. A randomized, controlled trial of 3.0 mg of liraglutide in weight management. New England Journal of Medicine 373:11–22.

[97] Williams, D.L., Baskin, D.G., Schwartz, M.W., 2006. Leptin regulation of the anorexic response to glucagon-like peptide-1 receptor stimulation. Diabetes 55:3387–3393.

[98] Williams, D.L., Hyvarinen, N., Lilly, N., Kay, K., Dossat, A., Parise, E., et al., 2011. Maintenance on a high-fat diet impairs the anorexic response to glucagon-like-peptide-1 receptor activation. Physiology & Behavior 103: 557–564.

[99] Sandoval, D.A., Bagnol, D., Woods, S.C., D'Alessio, D.A., Seeley, R.J., 2008. Arcuate glucagon-like peptide 1 receptors regulate glucose homeostasis but not food intake. Diabetes 57:2046–2054.

[100] Hany, T.F., Gharehpapagh, E., Kamel, E.M., Buck, A., Himms-Hagen, J., von Schulthess, G.K., 2002. Brown adipose tissue: a factor to consider in symmetrical tracer uptake in the neck and upper chest region. European Journal of Nuclear Medicine and Molecular Imaging 29:1393–1398.

[101] Virtanen, K.A., Lidell, M.E., Orava, J., Heglind, M., Westergren, R., Niemi, T., et al., 2009. Functional brown adipose tissue in healthy adults. New England Journal of Medicine 360:1518–1525.

